Synthetic analogues of the parasitic worm product ES-62, reduce disease development in *in vivo* models of lung fibrosis

Colin J. Suckling[a], Sambuddho Mukherjee[b], Abedawn I. Khalaf[a], Ashwini Narayan[b], Fraser J. Scott[a], Sonal Khare[b], Saravanakumar Dhakshinamoorthy[b], Margaret M. Harnett[c] and William Harnett[d*]

[a]Department of Pure & Applied Chemistry, University of Strathclyde, Glasgow G1 1XL, UK

[b]Department of Discovery Biology, Jubilant Biosys Ltd, Bangalore-560022, India

[c]Institute of Infection, Immunity and Inflammation, University of Glasgow, Glasgow G12 8TA, UK

[d]Strathclyde Institute of Pharmacy and Biomedical Sciences (SIPBS), University of Strathclyde, Glasgow G4 0RE

*Corresponding Author: Prof. William Harnett, SIPBS, 161 Cathedral Street, University of Strathclyde, Glasgow G4 0RE, UK; e.mail: w.harnett@strath.ac.uk; phone: (0044)-141-548-3725

Abstract

Parasitic worms are receiving much attention as a potential new therapeutic approach to treating autoimmune and allergic conditions but concerns remain regarding their safety. As an alternative strategy, we have focused on the use of defined parasitic worm products and recently taken this one step further by designing drug-like small molecule analogues of one such product, ES-62, which is anti-inflammatory by virtue of covalently attached phosphorylcholine moieties. Previously, we have shown that ES-62 mimics are efficacious in protecting against disease in mouse models of rheumatoid arthritis, systemic lupus erythematosus and skin and lung allergy. Given the potential role of chronic inflammation in fibrosis, in the present study we have focused our attention on lung fibrosis, a debilitating condition for which there is no cure and which in spite of treatment slowly gets worse over time. Two mouse models of fibrosis - bleomycin-induced and LPS-induced - in which roles for inflammation have been implicated were adopted. Four ES-62 analogues were tested – **11a** and **12b**, previously shown to be active in mouse models of allergic and autoimmune disease and **16b** and **AIK-29/62** both of which are structurally related to **11a**. All four compounds were found to significantly reduce disease development in both fibrosis models, as shown by histopathological analysis of lung tissue, indicating their potential as treatments for this condition.

Keywords: drug development; fibrosis; ES-62; immunomodulation; parasitic worm

Abbreviations: ECM – extracellular matrix; PC – phosphorylcholine; SMA – small molecule analogue

1. Introduction

During the last few decades, a striking increase in the incidence of allergic and autoimmune conditions has been noted in urban areas of the world (reviewed by Bach, 2002). One hypothesis put forward to explain this is that decreased exposure to pathogens via for example, increased hygiene, use of antibiotics and vaccination, has resulted in the human immune system no longer being exposed to a range of organisms, which would normally impact on its development and regulation (the "Hygiene Hypothesis") (Strachan, 1989). Amongst these organisms, particular attention has been paid to parasitic worms, as examples of inverse correlations observed between the incidence of worm infection and conditions like rheumatoid arthritis (Panda et al., 2013; Panda and Das, 2016) and systemic lupus erythematosus (Panda and Das, 2016) are strongly supportive of a role for worms in protection against certain autoimmune conditions. The situation with respect to allergic conditions like asthma does not appear as clear-cut, with parameters such as species of worm parasite, parasite load and age of patient likely to play a role (reviewed by Santiago and Nutman, 2016). Nevertheless, mouse model studies of allergy reveal that a wide range of worm species, extracts of worms and defined individual worm products can protect against the development of disease (reviewed by Rzepecka and Harnett, 2014).

One particularly well-characterised worm product is ES-62, a secreted protein of the filarial nematode *Acanthocheilonema viteae*, which has anti-inflammatory properties by virtue of covalently attached phosphorylcholine (PC) residues (reviewed by Pineda et al., 2014). ES-62 is able to protect mice against ovalbumin-induced airway hypersensitivity in both acute (Melendez et al., 2007; Rzepecka et al., 2013) and chronic (Coltherd et al., 2016) models of airway hypersensitivity and protection in the chronic model is associated with reduction of airway remodeling. Pathological tissue remodeling is also a feature of fibrosis (reviewed by Duffield et al., 2013), a condition in which repetitive damage of tissue by some form of irritant results in dysregulation of the normal wound-healing response leading to deposition of extracellular matrix (ECM) and remodeled tissue. The previously characterized protective effects of ES-62 against

airway remodeling in the chronic ovalbumin-induced hypersensitivity model argue for assessment of its therapeutic potential against lung fibrosis. However, as a large, "foreign" protein it is potentially immunogenic and may have delivery-related issues. Hence, as an alternative approach we have generated a library of drug-like ES-62 small molecule analogues (SMAs) based around its active PC moiety (Al-Riyami et al., 2013). Our recent studies have investigated three SMAs termed **11a**, **12b** and **19o.** The first two compounds, like ES-62, are able to inhibit proinflammatory cytokine production by macrophages (Al-Riyami et al., 2013) and are protective in acute (Rzepecka et al., 2015a) and chronic (Coltherd et al., 2016) models of ovalbumin-induced airway hypersensitivity. Conversely **19o** was found to have no effect on macrophage cytokine production (Al-Riyami et al., 2013) and although it has not been tested in the asthma models, it was found, unlike **11a** and **12b,** to be unable to prevent spontaneous kidney disease development in the MRL/lpr mouse model of systemic lupus erythematosus (Rodgers et al., 2015). Our examinations to date indicate that active SMAs like 11a and 12b mimic a primary ES-62 mechanism of action in causing autophagolysosomal degradation of the TLR/IL-1R adaptor molecule MyD88 (Al-Riyami et al, 2013; Rzepecka et al, 2015b; Rodgers et al. 2015). Indeed, recently we have found that this reflects direct interaction between the SMAs and the TIR domain of MyD88 (Suckling et al. 2018).

The aim of this study was thus to test the two active SMAs – **11a** and **12b** - and also two further structurally-related SMAs, **16b** and **AIK-29/62**, against development of pulmonary fibrosis in two distinct mouse models – LPS and bleomycin-induced fibrosis. Bleomycin is a cytostatic drug and a chemotherapeutic antibiotic produced by the bacterium "*Streptomyces verticillus*" that is commonly employed in the treatment of cancer. As a side effect of its therapeutic use, repeated systemic administration of bleomycin induces chronic pulmonary inflammation in some patients that may progress to fibrosis (Moeller et al., 2008). Bleomycin causes injury which follows a pattern of acute neutrophilic inflammation and disruption of the alveolar capillary barrier that usually peaks between days 3–7, followed by resolution of inflammation and

development of a fibroproliferative phase. Bleomycin-induced pulmonary fibrosis is a well-established disease model for idiopathic pulmonary fibrosis and widely used in the investigation of therapeutic molecules. LPS, an endotoxin of Gram-negative bacteria is known to cause acute lung injury (ALI). LPS exerts its biological effects through Toll-like receptor 4 (TLR4) and promotes secretion of pro-fibrotic cytokines, including transforming growth factor-β1 (TGF-β1). LPS stimulation eventually results in the deposition of extracellular matrix (ECM): of note, therefore, we have previously found two of the ES-62 SMAs employed in the current study, **11a** and **12b**, to interfere with LPS-induced pro-inflammatory responses (e.g. cytokine production) by macrophages (Al-Riyami et al., 2013) and dendritic cells (Lumb et al., 2017) *in vitro*.

2. Materials & Methods

2.1 Experimental Animals

Female C57BL/6 mice (10-11 week old), with body weight range of 17-21 grams were procured from Charles River (USA). Animals were housed under standard specific pathogen-free conditions in vented cages. A single comprehensive experiment, comprising LPS- and Bleomycin-induced fibrosis models, was conducted according to protocols approved by IAEC (Institutional Animal Ethics Committee), IAEC/JDC/2014/54 at Jubilant Biosys, with mice acclimatized to these conditions for two weeks prior to dosing. Mice were randomized based on body weight, into groups (n=5/6 per group) such that mean body weights of animals in different groups were not statistically significant and variations within a group spanned less than 20%.

2.2 Chemicals

Bleomycin sulphate was purchased from Alfa Aesar (J60727); LPS (*E. coli* serotype 055:B5; L2880), dexamethasone (dimethyl sulfoxide (DMSO) soluble), pepsin, DMSO, bovine serum albumin (BSA) and phosphate buffered saline (PBS) were purchased from Sigma. Bleomycin sulphate (50 µg per mouse) and LPS (40 µg per mouse) were prepared by dissolving in PBS immediately prior to use. ES-62 SMAs used in this investigation were **11a**, **12b**, **16b** and **AIK-29/62** and each was synthesised at the University of Strathclyde. **11a, 12b**, and **16b** have been described and employed previously (Al-Riyami et al., 2013; Rzepecka et al., 2015a); **AIK-29/62** is a new compound (Fig. 1). The main stocks (100 mg/ml) were prepared in DMSO (D2650, Sigma) and stored at -80°C. The SMA sub-stocks (1 mg/ml) were prepared in DMSO and were stored in 4°C until use. At the time of the experiments, the SMAs were diluted 1:200 with PBS and a dose volume of 200 µl injected subcutaneously on the scruff of the neck. The same DMSO concentration (0.5%) was maintained in the control PBS ("Vehicle") group. Dexamethasone 0.4 mg/kg was prepared in PBS and injected by the intra-peritoneal route, as an internal disease protection control.

2.3 Sirius red Collagen assay

The Sirius Red Collagen Detection Kit (catalog no. 9062) was purchased from Chondrex Inc, USA) and the assay was performed as per manufacturer's instructions. Briefly, the left lobe of the lung (superior & inferior left lobe) was collected and flash frozen immediately in a sterile pre-weighed 1.5 ml Eppendorf tube containing 2 metal beads of 4 mm thickness and stored at -80°C until processed. For processing the samples, 300 µl of milli-Q water was added to promote lysis. Tissue lysis was performed on a pre-chilled metal block in a Geno grinder (Geno / Grinder® SPEX Sample Prep P 2010) at 900 rpm for 2 min for 4 cycles. Pepsin (100 µl; from porcine gastric mucosa, P7000, Sigma) prepared as 1 mg/ml in 0.05 M acetic acid (supplied in Chrondrex Kit) was added to each sample tube. The contents were gently mixed and incubated overnight at 4°C in an end-to-end rotor, with ~20 µl of sample removed for protein estimation using the Bradford reagent from Biorad. The following day samples were centrifuged at 8,000 rpm for 10 min before transfer of 250 µl of the clear supernatant into a clear 1.ml Eppendorf tube. Sirius Red solution (500 µl) was added to the supernatant, and the sample vortexed and incubated overnight at 4°C. Collagen standards (starting conc. of 500 µg/ml) were prepared in 0.05% acetic acid as per manufacturer's instructions, with 100 µl of standard solutions transferred into fresh tubes. Sirius Red solution (500 µl) was added to all the standard tubes, which were then vortexed and incubated overnight at 4°C. The next day standards and samples were centrifuged at 10,000 rpm for 25 minutes at 4°C and the supernatant discarded carefully without disturbing the pellet. The pellet was washed twice using 500 µl of wash solution before addition of 250 µl of extraction buffer and vortexing to completely dissolve the pellet. Samples (200 µl) were transferred to a 96-well plate, and the OD read at 510-550 nm.

2.4 Histopathological evaluation

Mouse lung (right inferior lobe) tissues were processed for routine paraffin embedding and serial sections of 6 µm thickness were prepared. Slides were stained with

hematoxylin and eosin (H & E) for detailed examination of tissue pathology whilst the Richard Allan Gomori Trichrome staining kit (Thermo Scientific) was employed to assess the collagen content, visualised as blue fibers. The extent of disease severity was assessed using the modified Ashcroft scale (Hubmer et al., 2008) where the entire lung section was examined for pulmonary fibrotic changes and sections representative of the scoring system are shown in Fig. 2. This clinical scoring reflects the extent and severity of cellularity in the alveolar wall (interstitium); metaplastic cells lining the air spaces, including foci of honeycomb lung; the extent and severity of cellularity in the alveolar space (desquamation); interstitial “young connective tissue” interstitial fibrosis; honeycomb cysts; metaplastic smooth muscle in the stroma; myointimal mural thickening in the vessel walls; airway luminal granulation tissue; air space granulation tissue; airway wall inflammation; airway wall fibrosis, as indicated.

2.5 Study Protocol

This study comprised a single experiment with two arms, with the objectives being the investigation of bleomycin-and LPS-induced lung fibrotic changes. 70 animals were procured and randomized based on the study plan. Pulmonary fibrosis was induced either by a single dose of oropharyngeal instillation with 50 µg bleomycin sulphate (dissolved in 40 µl of PBS) or 40 µg of LPS (dissolved in 40 µl of PBS). Mice that were injected with PBS served as controls. The four test compounds were dosed at 0.05 mg/kg and dexamethasone at 0.4 mg/kg. Animals from respective treatment groups were administered with vehicle or test compound/dexamethasone for 6 days a week and dexamethasone thrice weekly starting from day 0 to 7 for the LPS group and day 0 to 13 for the bleomycin group. Mortality (if any), clinical signs, and body weight (3-4 days weekly) were recorded. The animals were sacrificed on day 8 (LPS group) or day 14 (bleomycin group), time-points chosen on the basis of our previous experiments analysing collagen deposition. Lung lobes were sampled according to the relevant assays (left lung lobes: superior and inferior for collagen assay; right superior and middle lobe as reserve and right inferior lobe for histopathology analysis) and tissue

weights were recorded. Lung lobes were analyzed for collagen levels and histopathological analysis. One mouse from the bleomycin-treated cohort was found dead on Day 12, presumably due to disease severity. One animal each from dexamethasone-treated (bleomycin-induced) and AIK-29/62 treated (LPS-induced) groups were found dead on the day of sensitization (day 0), presumably due to the challenges in recovery from anesthesia.

2.6 Statistical Analysis

All statistical analyses were performed using Graphpad Prism software, using a one-way ANOVA or 2-way ANOVA analysis and Fisher's least significance difference post-test or Kruskal Wallis post-test where stated for the Ordinal Histopathology data.

3. Results

3.1 Histopathological assessment of effect of ES-62 SMAs in models of lung fibrosis

A single comprehensive experiment was undertaken involving the use of two different fibrosis models - LPS- and bleomycin-induced - and four distinct SMAs. Histopathological analysis of lung tissues revealed that lung parenchyma of LPS and bleomycin disease groups display significant pathology with development of alveolar septa, widening and disturbance of alveolar structure, severe inflammatory cell infiltration, and excessive collagen deposition. By contrast, mice treated with **11a**, **12b**, **16b**, **AIK-29/62** or dexamethasone showed substantial protection from LPS- and bleomycin-induced damage such as reduction in each of alveolar septa widening, inflammatory cell infiltration, fibroblast proliferation and excessive collagen deposition (Fig. 3A). Supporting this, the scoring of disease severity showed that whilst both the LPS- and Bleomycin-disease groups have scores significantly different to those of the vehicle mice, none of the treated groups (**11a**, **12b**, **16b**, **AIK-29/62** or dexamethasone) displayed scores significantly different from the healthy mice (Fig. 3B).

3.2 Effect of ES-62 SMAs on body weight and lung tissue weight in models of fibrosis

Following an initial drop in body weight following treatment with LPS, the animals generally recovered over the duration of the experiment and ultimately, the administered compounds had little effect on the weight of the animals (Fig. 4). Treatment with bleomycin showed some evidence of causing a reduction in body weight although this did not reach statistical significance. Relative to the no disease control group, all of the LPS-treatment groups showed slightly elevated dry lung weights, which were not significantly decreased by any of the interventions, although those treated with AIK-29/62 or dexamethasone were not significantly different from healthy controls. The lung tissue weights of diseased animals in the bleomycin groups treated with PBS, 11a or 12b were also significantly higher when compared to the control group whereas treatment with each of SMA **16b** and **AIK-29/62** suppressed this (Fig. 5). Indeed, the

lung weights of these two treatment groups and in addition dexamethasone were not significantly different from healthy controls.

3.3. Effect of ES-62 SMAs on collagen deposition in models of fibrosis

Fibrosis results from an abnormal wound-healing response following alveolar injury forming a scar. The fibroblasts involved in scarring have a myofibroblast phenotype characterized by α-smooth muscle actin (α-SMA) expression and increased secretion of collagen types I and III. The collagen content in fibrotic tissues was estimated using Sirius Red dye, which specifically binds to the [Gly-X-Y]n helical structure on fibrillar collagen (type I to V) but does not discriminate between collagen species and types.

Collagen levels were estimated from the left superior and inferior lobes of mice and expressed as micrograms of collagen per milligram tissue (µg/mg). LPS and bleomycin both significantly increased the levels of collagen detected: administration of 0.05 mg/kg of compound **AIK-29/62** or dexamethasone attenuated collagen deposition in the LPS-treated mice as shown by statistically significant differences from the LPS-PBS control (Fig. 6). The other treatments had no statistically significant effect and likewise, none of the treatments were able to prevent bleomycin-induced collagen deposition.

4. Discussion

Fibrosis, or scarring, is defined by the accumulation of excess extracellular matrix (ECM) components such as collagen and fibronectin in and around the inflamed or damaged area which can further lead to permanent scarring, organ malfunction and ultimately death (reviewed by Duffield et al., 2013). In this study, we investigated the protective effects of synthetic SMAs of the immunomodulatory parasitic worm product ES-62 against fibrosis. These SMAs are drug-like compounds that have previously been shown to protect against inflammatory exacerbations in an ovalbumin-dependent model of chronic asthma (Coltherd et al., 2016).

As expected, both bleomycin and LPS caused fibrosis to develop in the lungs of treated mice. SMAs **11a** and **12b,** when tested in quantities analogous to those previously shown to protect against disease development in models of allergy and autoimmunity (Al-Riyami et al., 2013; Rzepecka et al., 2015a; Rzepecka et al., 2015b), were able to significantly reduce this and to a level comparable to the disease-active control compound, dexamethasone. The two compounds new to *in vivo* evaluation, SMAs **16b** and **AIK-29/62**, are structurally related to SMA **11a** and they too behaved in a similar manner to dexamethasone when tested in the model. **12b** is rather different in chemical structure, being the only one of the four SMAs evaluated that can readily form a vinyl sulfone. As we discussed previously (Rzepecka et al., 2015b), because a vinyl sulfone has potential for additional biological activity to that related to ES-62 it is possible that this could contribute to the observed behavior of **12b** in not reducing collagen deposition. In any case, all four compounds showed therapeutic potential for the treatment of fibrosis. Caution should be observed with respect to **AIK-29/62** as there is some indication that it may be enhancing the reduction in body weight observed when employing bleomycin, although this was not statistically significant by the end of the experiment. At the same time, however, SMAs **AIK-29/62** and **16b** were able to significantly inhibit the observed increase in lung tissue weights observed in bleomycin-treated groups.

To investigate their mechanism of action, we also measured the amount of collagen present in the lungs: whilst both LPS and bleomycin significantly increased collagen levels, only SMA **AIK-29/62** and dexamethasone were able to significantly prevent this and only with respect to LPS treatment. Interestingly however, SMAs 11a and 16b also showed a reduction in the LPS model but this did not reach statistical significance. The undertaking of further experiments, by increasing the power of the analysis, could perhaps confirm whether they are truly having an effect in reducing collagen deposition. In any case, relating to this general absence of a significant effect with the SMAs, we had previously subjected **12b-**exposed bone marrow-derived macrophages to microarray analysis (Rzepecka et al. 2015b) and noted no effect on expression of collagen genes such as col1a2 and col3a1. At the same time however, 9 of the genes present in the mouse fibrosis PCR array produced by Quiagen were affected. In eight of these cases the change was in a direction likely to inhibit fibrosis. Thus, there is decreased expression of the genes corresponding to 6 mediators that play a role in pulmonary fibrosis – CCR2 (Moore et al. 2001) – expression reduced 3.8-fold; IL-1β (Borthwick, 2016) – expression reduced 8.9-fold (most affected gene in the study); PDGFB (Abdollahi *et al.,* 2005) – expression reduced 2.1-fold; TGFB1 Fernandez and Eickelberg, 2012) – expression reduced 1.6-fold; TGFB3 (Emblom-Callahan et al., 2010) – expression reduced 2.1-fold and NFκB1 (Christman, Sadikot and Blackwell, 2000) – expression reduced 1.8-fold. At the same time, there is increased expression (2.9-fold) of Mmp13, an enzyme found to limit the overall magnitude of ECM build up in the fibrotic lung (Nkyimbeng et al., 2013) and uPa (2.6-fold), which would be expected to result in increased collagen degradation and tissue fibrogenesis (Ghosh and Vaughan, 2012) The only gene that showed a change in expression that is perhaps more difficult to reconcile with a protective role against fibrosis is CCL3 L1/L3 (1.7-fold increase) as the chemokine CCL3 is considered to play a role in promoting fibrosis (Yang et al. 2011). Overall however, the changes in gene expression are clearly consistent with a protective effect against fibrosis and thus mirror the protective effects shown in the present study.

In summary, parasitic worm products are increasingly being considered as novel therapeutics for human illnesses associated with aberrant inflammatory responses (reviewed by Rzepecka and Harnett, 2014). We have recently taken this a step further via the production of synthetic drug-like SMAs of one of the best characterized of these molecules, ES-62 (Al-Riyami et al., 2013). In the current study, we demonstrate that these SMAs are effective in modulating key efficacy markers in a subset of fibrotic diseases. It should be noted however that a limitation of the study is that it comprises a single experiment. Although this was comprehensive, involving the use of two different fibrosis models and four distinct SMAs and with a sufficient number of animals per group to achieve statistical significance, the undertaking of further experiments will be necessary to confirm the existence of the protective effect and also to determine whether it is present in a therapeutic setting. Certainly, at this stage the SMAs appear to offer a novel approach to the treatment of fibrosis, a debilitating condition for which current therapies remain inadequate. With respect to obtaining a candidate drug based upon these and cited results, SMAs **11a** and **12b** do not have hERG or CYP inhibition liabilities but optimization will be required in terms of pharmacokinetic properties and dosing regime, for the treatment of fibrosis or other appropriate diseases.

Funding: This research did not receive any specific grant from funding agencies in the public, commercial, or not-for-profit sectors.

5. References

Abdollahi, A. et al. (2005) Inhibition of platelet derived growth factor signaling attenuates pulmonary fibrosis. *Journal of Experimental Medicine* 201, 925-935.

Al-Riyami, L., Pineda, M.A., Rzepecka, J., Huggan, J.K., Khalf, A.I., Suckling, C.J., Scott, F.J., Rodgers, D.T., Harnett, M.M. and Harnett, W. (2013) Designing anti-inflammatory drugs from parasitic worms: a synthetic small molecule analogues of the *Acanthocheilonema viteae* product ES-62 prevents development of collagen-induced arthritis. *Journal of Medicinal Chemistry* 56, 9,982-10,002.

Bach, J.F. (2002) The effect of infections on susceptibility to autoimmune and allergic diseases. *New England Journal of Medicine* 347, 911-920.

Borthwick, L.A. (2016) The IL-1 cytokine family and its role in inflammation and fibrosis in the lung. *Semin. Immunopathol*. 38, 517-534.

Christman, J.W., Sadikot, R.T. and Blackwell, T.S. (2000) The role of nuclear factor-κB in inflammatory diseases. *Chest* 117, 1,482-1,487.

Coltherd, J.C., Rodgers, D.T., Lawrie, R.E., Al-Riyami, L., Suckling, C.J., Harnett, W. and Harnett, M.M. (2016) The parasitic worm-derived immunomodulator ES-62 and its drug-like small molecule analogues exhibit therapeutic potential in a model of chronic asthma. *Scientific Reports*, January 14, e.publication.

Duffield, J.S., Lupher, M., Thannickal, V.J. and Wynn, T.A. (2013) Host responses in tissue repair and fibrosis. *Annual Review of Pathology* 8, 241-276.

Emblom-Callahan, M.C. et al. (2010) Genomic phenotype of non-cultured plulmonary fibroblasts in idiopathic pulmonary fibrosis. *Genomics* 96, 134-145.

Fernandez, I.E. Eickelberg, O. (2012) The impact of TGF-β on lung fibrosis. *Proc. Am. Thorac. Soc.* 9, 111-116.

Ghosh, A.K and Vaughan, D.E. (2012) PAI-1 in tissue fibrosis. *J Cell. Physiol*. 227, 493-507.

Hubner, R.H., Gitter, W., El Mohktari, N.E., Mathiak, M., Both, M., Bolte, H., Freitag-Wolf, S. and Bewig, B. (2008) Standardised quantification of pulmonary fibrosis in hstological samples. *Biotechniques* 44, 507-511.

Lumb, F.E., Doonan, J., Bell, K.S., Pineda, M.A., Corbet, M., Suckling, C.J., Harnett, M.M. and Harnett, W. (2017) Dendritic cells provide a therapeutic target for synthetic small molecule analogues of the parasitic worm product, ES-62. *Scientific Reports,* May 10, e.publication.

Melendez, A.J., Harnett, M.M., Pushparaj, P.N., Wong, W.S., Tay, H.K., McSharry, C.P. and Harnett, W. (2007) Inhibition of FcεRI-mediated mast cell responses by ES-62: a product of parasitic filarial nematodes. *Nature Medicine* 13: 1,375-1,381.

Moeller, A., Ask, K., Warburton, D., Gauldie, J. and Kolb, M. (2008) The bleomycin animal model: a useful tool to investigate treatment options for idiopathic pulminary fibrosis? *International Journal of bIochemistry and Cell Biology* 40, 362-382.

Moore, B.B., Paine III, R., Christensen, P.J., Moore, T.A., Sitterding, S., Ngan, R., Wilkie, C.A., Kuziel, W.A. and Toews, G.B. (2001) Protection from pulmonary fibrosis in the absence of CCR2 signaling. Journal of Immunology 167, 4,368-4,377.

Nkyimebeng, T. et al. (2013) Pivotal role of matrix metalloproteinase 13 in extracellular matrix turnover in idiopathic pulmonary fibrosis. PLOS One, e73279.

Panda, A.K. and Das, P.K. (2016) diminished IL-17A levels may protect filarial-infected individuals from development of rheumatoid arthritis and systemic lupus erythematosus. *Lupus*, August 3, e.publication.

Panda, A.K., Ravindran, B. and Das, B.K. (2013) Rheumatoid arthritis patients are free of filarial infection in an area where filariasis is endemic: comment on the article by Pineda et al. *Arthritis and Rheumatism* 64, 1,402-1,403.

Pineda, M.A., Lumb, F., Harnett, M.M. and Harnett, W. (2014) ES-62, a therapeutic anti-inflammatory agent evolved by the filarial nematode *Acanthocheilonema viteae*. *Molecular and Biochemical Parasitology* 194: 1-8.

Rodgers, D.T., Pineda, M.A., Suckling, C.J., Harnett, W. and Harnett, M.M. (2015) Drug-like analogues of the parasitic worm-derived immunomodulator ES-62 are therapeutic in the MRL/lpr model of systemic lupus erythematosus. *Lupus* 24, 1437-1442.

Rzepecka, J., Coates, M.L., Saggar, M., Al-Riyami, L., Coltherd, J., Tay, H.K., Huggan, J.K., Janicova, L., Khalaf, A.I., Siebeke, I., Suckling, C.J., Harnett, M.M. and Harnett, W. (2015a) Small molecule analogues of the immunomodulatory parasitic helminth product have anti-allergy properties. *International Journal for Parasitology* 44, 669-674.

Rzepecka, J. and Harnett, W. (2014) Can the study of helminths be fruitful for human diseases? In: Helminth infections and their impact on global public health". Ed: Bruschi, F. Springer, Wein. pp. 479-502.

Rzepecka, J., Pineda, M.A., Al-Riyami, L., Rodgers, D.T., Huggan, J.K., Lumb, F.E., Khalaf, A.I., Meakin, P.J., Corbet, M., Ashford, M.L., Suckling, C.J., Harnett, M.M. and Harnett, W. (2015b) Prophylactic and therapeutic treatment with a synthetic analogue of a parasitic worm product prevents experimental arthritis and inhibits IL-1b production via NRF2-mediated counter-regulation of the inflammasome. *Journal of Autoimmunity* 60, 59-73.

Rzepecka, J., Siebeke, I., Cotlherd, J.C., Kean, D.E., Steiger, C.N., Al-Riyami, L., McSharry, C. P., Harnett, M.M. and Harnett, W. (2013) The helminth product ES-62 protects against airway inflammation by resetting the Th cell phenotype. *International Journal for Parasitology* 43: 211-223.

Santiago, H.C. and Nutman, T.B. (2016) Human helminths and allergic disease: the hygiene hypothesis and beyond. *American Journal of Tropical Medicine and Hygiene* 95, 746-753.

Strachan, D.P. (1989) Hay fever, hygiene and household size. *British Medical Journal* 299, 1,259-1,260.

Suckling, C.J., Alam, S., Olson, M.A., Saikh, K.U., Harnett, M.M. and Harnett, W. (2018) Small molecule analogues of the parasitic worm product ES-62 interact with the TIR domain of MyD88 to inhibit proinflammatory signaling. *Scientific Reports*, 8(1):2123.

Yang, X. et al. (2010) The chemokine, CCL3, and its receptor, CCR1, mediate thoracic radiation-induced pulmonary fibrosis. *Am. J. Respir. Cell. Mol. Biol.* 45, 127-135.

Figure Legends

Fig. 1. Structures and properties of the ES-62 SMAs.

Code	Structure	MW/Formula
AIK-29/62	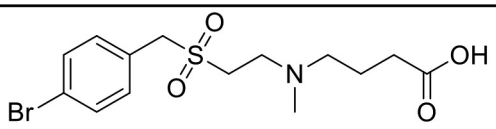	378.28 $C_{14}H_{20}BrNO_4S$
11a [S3]	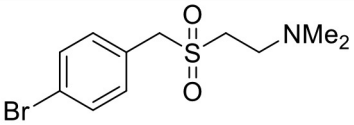	305.01 $C_{11}H_{16}BrNO_2S$
12b [S5]	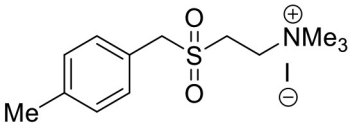	383.04 $C_{13}H_{22}INO_2S$
16b	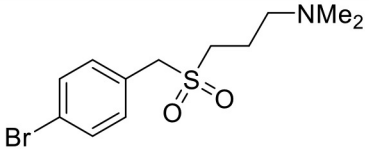	320.25 $C_{12}H_{18}BrNO_2S$
Prototype **PC-ES-62**	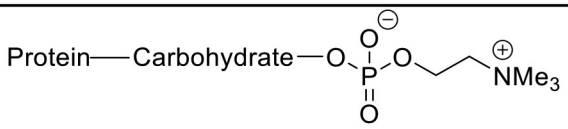	

Fig. 2. Representative images of the clinical scoring of fibrosis from LPS and Bleomycin treated groups. Lung histology shows H & E staining (left panels; 10X magnification) and Trichrome Gomori staining (right panels; 10X magnification; collagen is stained in blue). Scores 0, 1, 2, 3, 5 and 6 represent increases in disease severity. Slides with a score of 0, 3, and 5 are from the LPS-treated group, whilst those with a score of 1, 2, and 6 are from the Bleomycin treatment group. In this study, we did not find tissue exhibiting a score representative of 4.

Score	H & E	Trichrome Gomori	
0	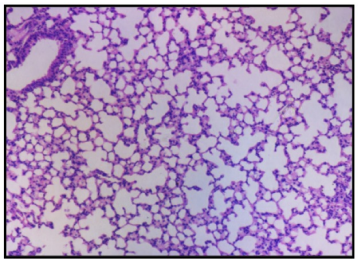	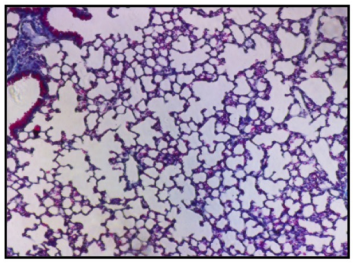	Normal lung
1	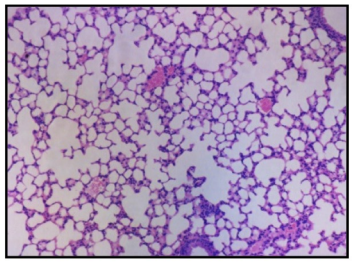	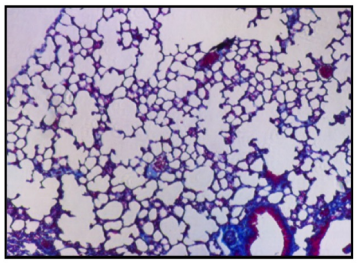	Gentle fibrotic changes, alveoli partly enlarged
2	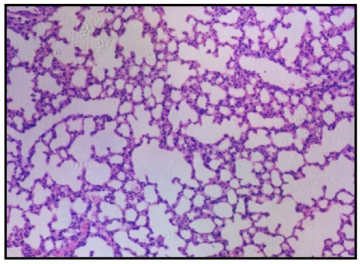	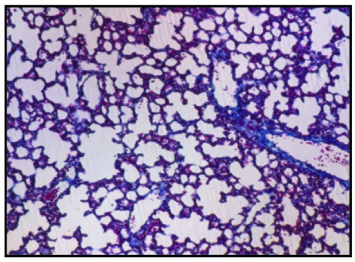	Knot-like formation
3	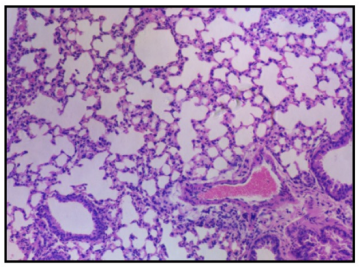	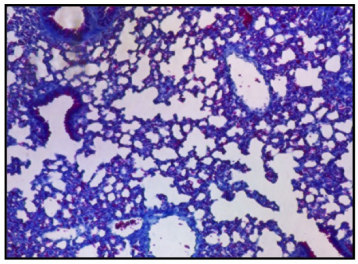	Continuous fibrotic walls, alveoli partly enlarged
5	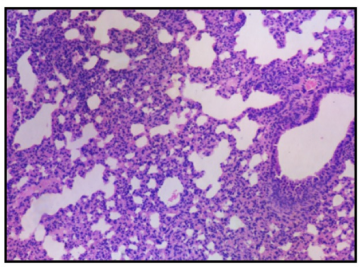	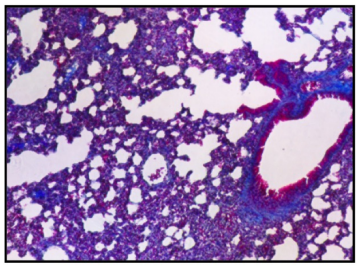	Variable alveolar septa, confluent fibrotic mass, lung structure damaged in 10-50% of microscopic field
6	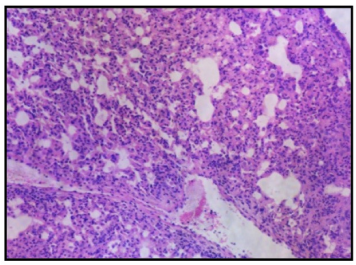	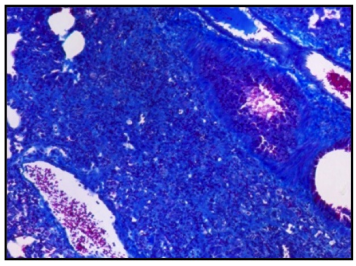	Alveloar septa mostly not existent, continuous fibrotic mass in >50% of field

Fig. 3. Protection against fibrosis by SMAS 11a, 12b, 61 and AIK-29/62. A. Lung histology shows 2 representative images of Trichrome Gomori (10X magnification) staining of the lungs from each group. Excessive collagen deposition and inflammatory cell infiltration were visible in the disease groups. **B.** Lung histopathological scores of the groups where data are represented as median ± interquartile range values (n=5 LPS [except 62, n=4]; n=6 bleomycin [except PBS n=5 and dexamethasone (Dex) n=4]). Analysis by 1-way ANOVA and Kruskal Wallis post-test showed that LPS and bleomycin induce significant increases (*$p<0.05$; **$p<0.001$) in disease severity compared to the no-disease control group (Vehicle) and #, ## denotes the significant decrease (#$p<0.05$, ##$p<0.01$) in disease severity resulting from treatment with the SMAs compared to the disease control (PBS) group. AIK-29/62 is denoted by “62”. None of the animals treated with the SMAs or dexamethasone showed scores significantly different to the healthy control cohort.

A.

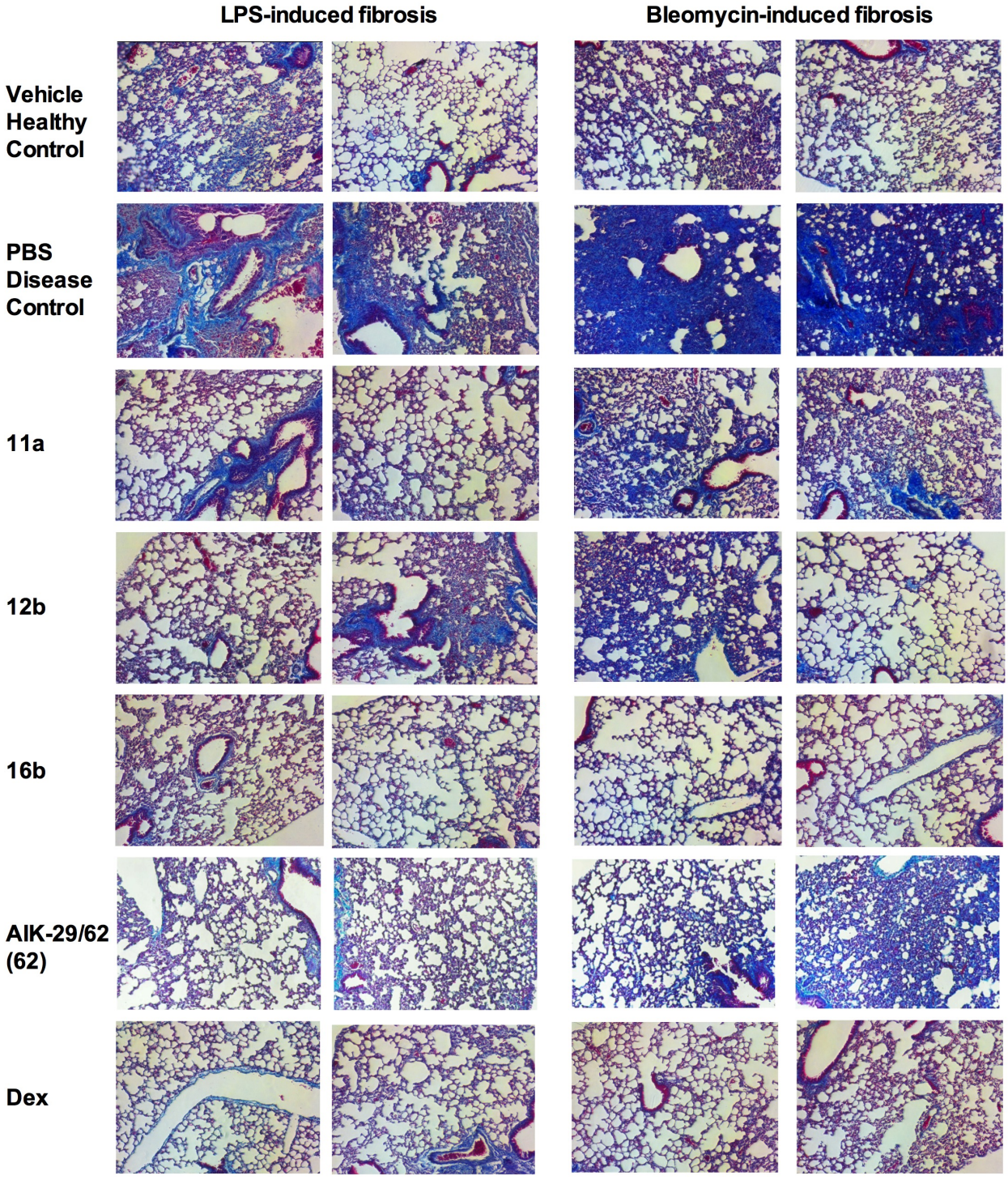
LPS-induced fibrosis
Bleomycin-induced fibrosis
Vehicle Healthy Control
PBS Disease Control
11a
12b
16b
AIK-29/62 (62)
Dex

B.

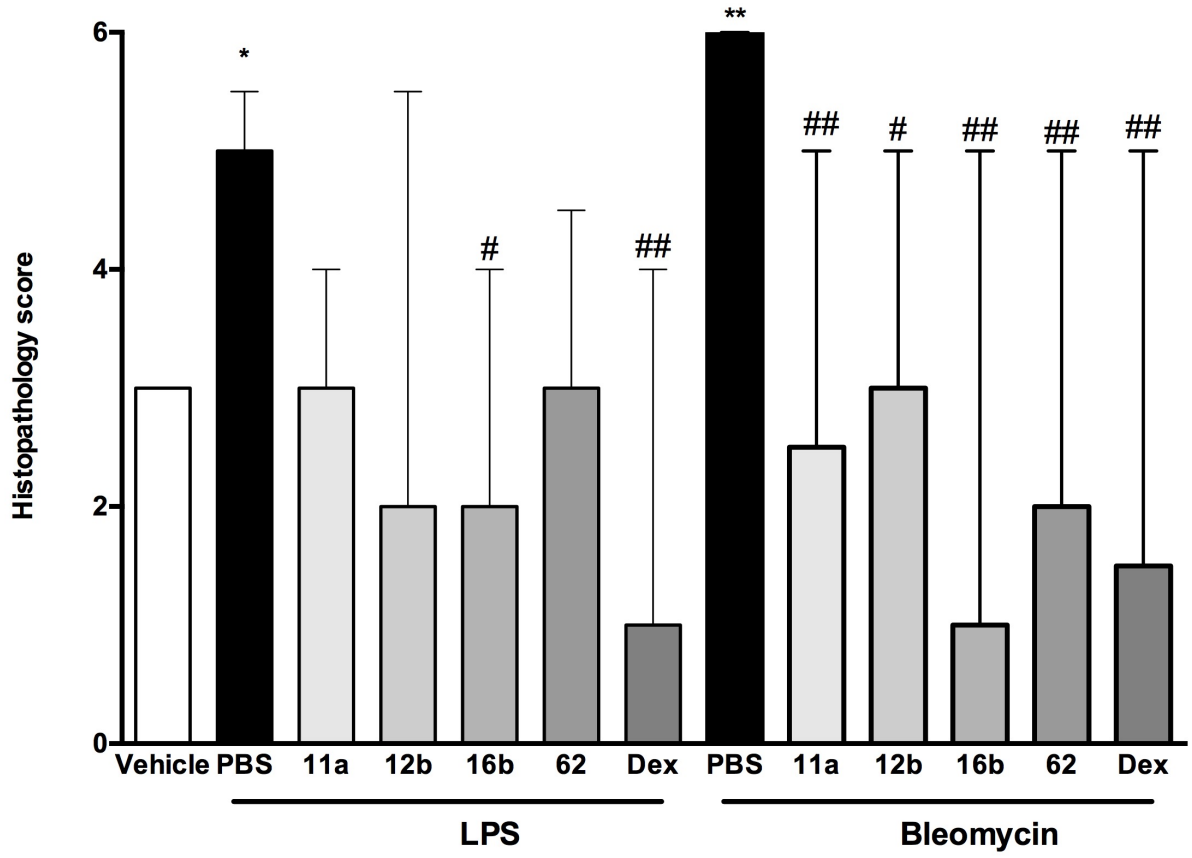
Histopathology score
6
4
2
0
*
**
#
##
##
#
##
##
##
Vehicle
PBS
11a
12b
16b
62
Dex
PBS
11a
12b
16b
62
Dex
LPS
Bleomycin

Fig. 4: **Body weight representation from LPS (A) and Bleomycin (B) groups.** Data are presented as mean ± SEM (n=5 for LPS groups, except for “62” group n=4; n=6 for bleomycin groups, except for PBS group n=5 and for Dex group n=4). Data were analysed by 2-way ANOVA.

For LPS:

Day 1: ***p<0.001 for LPS + PBS, LPS + **11a**, LPS + **12b**, LPS + **16b**; **p<0.01 for LPS + **AIK-29/62** (denoted by “62”) and *p<0.05 for LPS + Dex, all versus Vehicle, i.e., no LPS-induced disease

Day 3: **p<0.01 for LPS + PBS and *p<0.05 for LPS + **11a**, LPS + **12b**, LPS + **16b,** all versus Vehicle

Day 8: *p<0.05 for LPS + PBS and LPS + Dex, versus Vehicle

For bleomycin

Day1: *p<0.05 for bleomycin + **16b** and bleomycin + **AIK-29/62 (**denoted by “62”.) versus Vehicle, i.e., no bleomycin-induced disease

Day 3: *p<0.05 for bleomycin + **AIK-29/62 (**denoted by “62”) versus Vehicle

Day 6: *p<0.05 for bleomycin + **AIK-29/62 (**denoted by “62”) versus Vehicle)

Day 8: *p<0.05 for blemycin + PBS, bleomycin + **11a**, blemycin + 1**2b**, bleomycin + Dex and ***p<0.001 for bleomycin + **AIK-29/62** (denoted by “62”) versus Vehicle.

A.

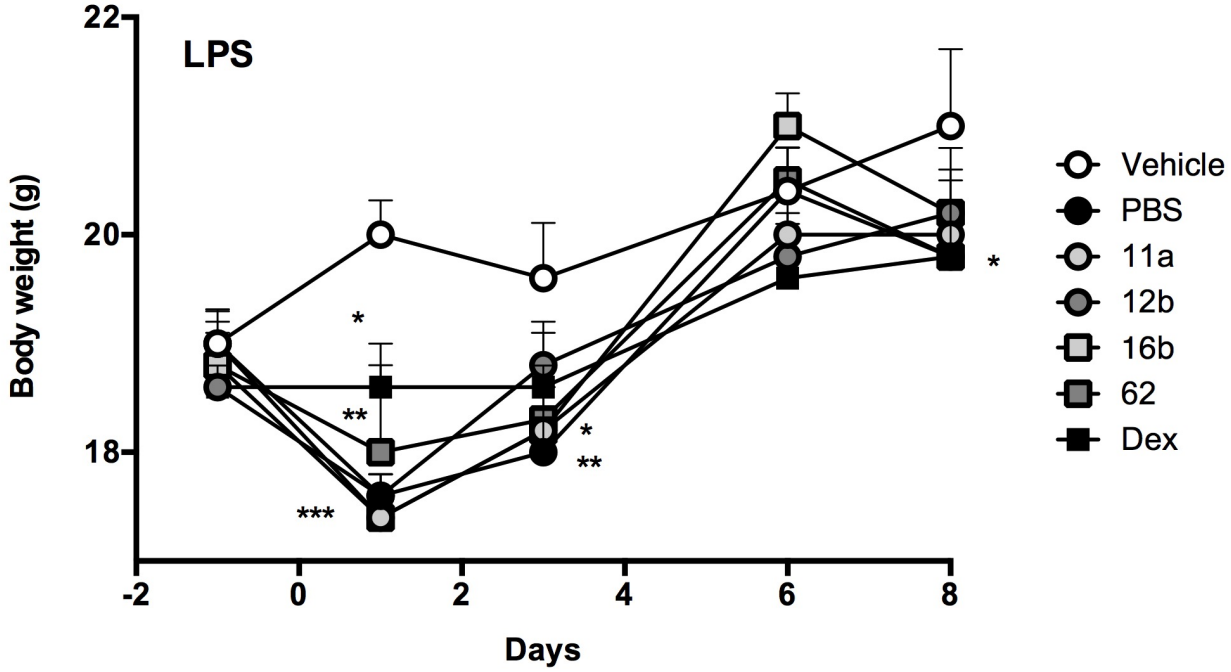
LPS
Body weight (g)
22
20
18
-2
0
2
4
6
8
Days
Vehicle
PBS
11a
12b
16b
62
Dex

B.

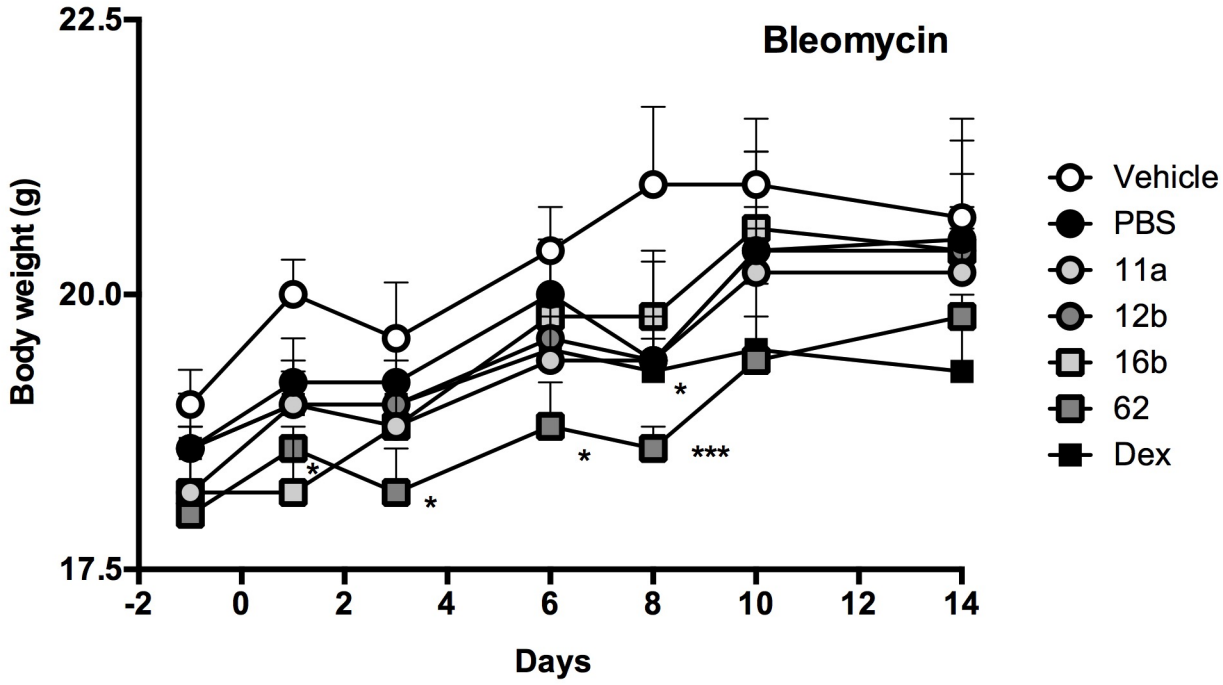
Bleomycin
Body weight (g)
22.5
20.0
17.5
-2
0
2
4
6
8
10
12
14
Days
Vehicle
PBS
11a
12b
16b
62
Dex

Fig. 5: Tissue weights of left lung lobe from LPS- and bleomycin-groups. Data are represented as mean ± SEM (n=5 LPS, except for **AIK-29/62** [denoted by "62", n=4] as one-treated mouse died on d1; n=6 bleomycin, except for PBS=5 as one mouse died on d13 and for Dex =4 as one mouse died on d1). Significant increases (*p<0.05; **p<0.01 and ***p<0.001) in tissue weight compared to Vehicle are indicated whilst suppression of LPS- or bleomycin responses by treatments are denoted by #p<0.05 as analysed by 1-way ANOVA.

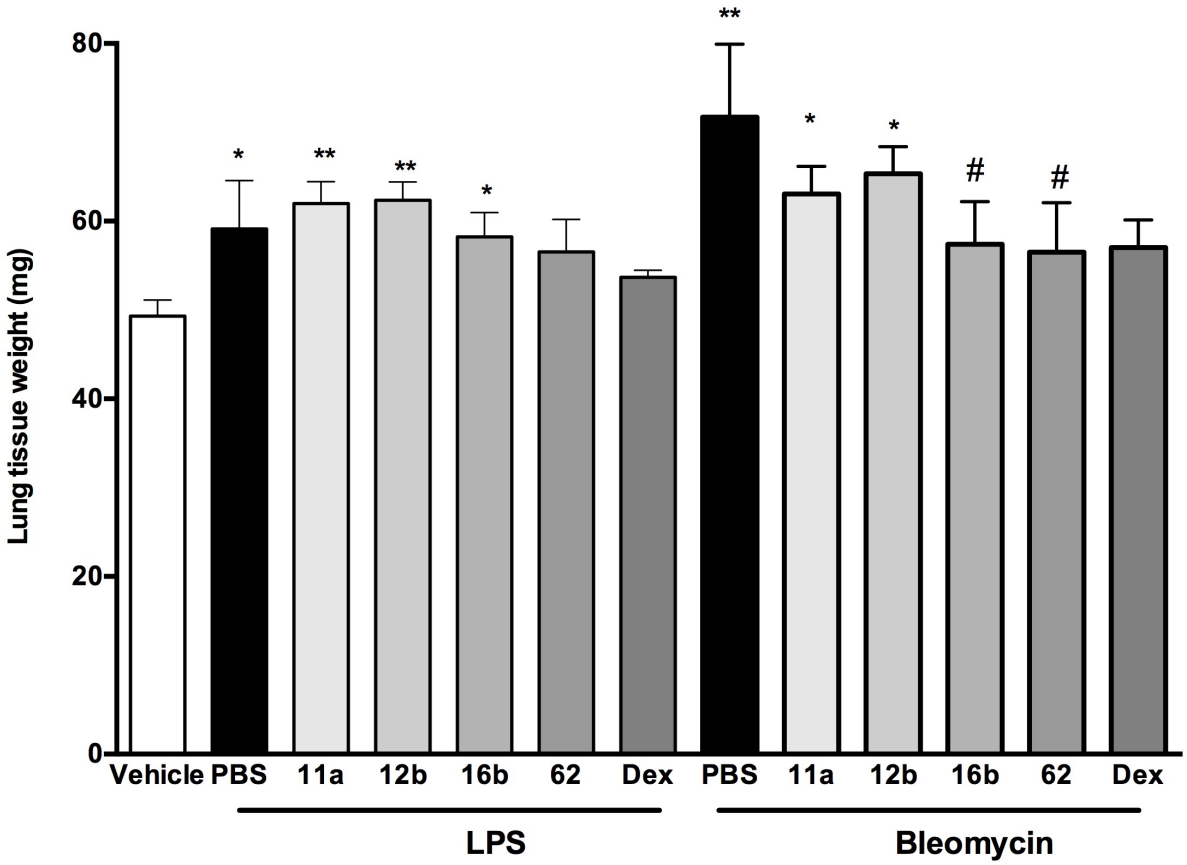

Fig. 6: Analysis of collagen concentration per left lung lobe from cohorts of LPS- and bleomycin-induced fibrosis, represented in µg per mg of lung tissue. Data are represented as mean ± SEM (n=5 LPS, except for **AIK-29/62** [denoted by "62", n=4] as one-treated mouse died on d1; n=6 bleomycin, except for PBS=5 as one mouse died d13 and for Dex =4 as one mouse died d1). Significant increases (*p<0.05; **p<0.01) compared to Vehicle are indicated whilst suppression of LPS- or Bleomycin responses by particular treatments are denoted by #p<0.05 as analysed by 1-way ANOVA.